ELSEVIER

Carbohydrate Polymers 46 (2001) 349–363

Carbohydrate Polymers

www.elsevier.com/locate/carbpol

# Structure and dynamics of the branched polysaccharide scleroglucan in dilute solutions studied by 1D and 2D NMR spectroscopy

S. Vlachou[a], A. Politou[a], P. Dais[a,*], K. Mazeau[b], F.R. Taravel[b]

[a]*NMR Laboratory, Department of Chemistry, University of Crete, 914 09 Iraklion, Crete, Greece*

[b]*Centre de Recherches sur les Macromolécules Végétales (CERMAV), Joseph Fourier University of Grenoble, CNRS, BP 53, 38041 Grenoble Cedex 9, France*

Received 7 July 2000; accepted 26 October 2000

**Abstract**

Variable temperature and magnetic field dependent $^{13}C$ NMR relaxation measurements ($T_1$ and NOE) were carried out for the branched polysaccharide scleroglucan in DMSO-$d_6$ dilute solutions. The relaxation data of the backbone carbons were analyzed quantitatively by using the bimodal time-correlation functions developed by Dejean, Lauprêtre, and Monnerie (DLM), which offered the best quantitative description of the segmental motion of the carbohydrate chains. Simple internal rotations of the free hydroxymethyl groups of the backbone rings about the exocyclic C-5–C-6 bonds superimposed on segmental motion have been described as a diffusion process of restricted amplitude. Multiple internal rotations involving the exocyclic hydroxymethyl group of the ring at the branched point and that of the side chain ring, as well as the side chain ring itself were described by employing a composite TCF for side chain motions superimposed on polymer segmental motions. These time-correlation functions and their Fourier transform pairs, the spectral densities, offered the best interpretation of the relaxation data of the exocyclic free hydroxymethyl groups, and the pendent D-glucorynosyl ring.

Finally, the $^{1}H$- and $^{13}C$ NMR spectra of the neutral scleroglucan in DMSO-$d_6$ were analyzed by employing a series of 2D NMR experiments. The 500 MHz $^{1}H$ NMR spectrum of scleroglucan at 283 K show severe peak overlaps, which do not allow the complete assignment of all signals in the carbon spectrum. 

*Keywords*: Scleroglucan; Time-correlation function; Spin–lattice relaxation

## 1. Introduction

Schleroglucan (**1**) is a branched polysaccharide of a regular structure comprising repeat units of four D-glucopyranosyl residues. One of these residues is β(1 → 6) linked to the main β(1 → 3) chain as a pendant group. Schleroglucan yields at low concentrations highly viscous aqueous solutions that have been used as thickeners in the food and pharmaceutical industries, while at higher concentrations schleroglucan forms gels. Moreover, scleroglucan is more soluble in dimethylsulfoxide solvent and basic aqueous solutions (pH ≥ 12).

X-ray diffraction studies (Bluhm, Deslandes, Marchessault, Perez & Rinaudo, 1982) and $^{13}C$ CP/MAS experiments (Bardet, Rousseau & Vincendon, 1993; Bluhm et al., 1982) have shown that scleroglucan adopts a triple helical (triplex) structure in the solid state. The triple helical conformation of scleroglucan is retained in aqueous solution (Bo, Milas & Rinaudo, 1987). However, no information is available in the literature about the dynamics of this polymer in solution. In order to obtain information about the flexibility (or rigidity) of the scleroglucan chain, we decided to perform variable temperature, multifield $^{13}C$ NMR relaxation experiments for this polysaccharide dissolved in the dimethylsulfoxide solvent. The choice of dimethylsulfoxide was dictated by the higher solubility of scleroglucan in this solvent, and by the fact that there are no interactions between the individual chains in dimethylsulfoxide (Rinaudo & Vincendon, 1982).

$^{13}C$ NMR relaxation measurements for each protonated carbon of the scleroglucan molecule requires first the assignment of the corresponding $^{13}C$ NMR spectrum. The assignment of the scleroglucan $^{13}C$ NMR spectrum in dimethylsulfoxide solutions has been attempted in an earlier publication (Rinaudo & Vincendon, 1982) in conjunction with spin–lattice relaxation measurements at 60°C and Larmor frequency of 62.9 MHz for the carbon nucleus. Although this NMR study confirmed the proposed chemical structure of this polysaccharide, the use of a relatively low magnetic field did not allow the complete resolution of all the signals in the spectrum (18 different signals were visible

* Corresponding author.
*E-mail address:* dais@chemistry.uch.gr (P. Dais).

0144-8617/01/$ - see front matter 
PII: S0144-8617(00)00334-9

in the spectrum out of a total of 24 signals). Moreover, spectral assignment was obtained by comparison of chemical shifts with the corresponding $\beta(1\rightarrow6)$ and $\beta(1\rightarrow3)$ linear homo-polysaccharides, the use of substituent parameters upon glycosylation, and when possible by comparing the measured spin–lattice relaxation times at different carbon sites. In an attempt to resolve as many as possible carbon resonances, we recorded a high-resolution $^{13}C$ NMR spectrum of scleroglucan at 100.5 MHz and at 283 K. This spectrum revealed 22 separate carbon resonances. Attempts have been made to analyze this spectrum by performing a number of two-dimensional (2D) NMR experiments.

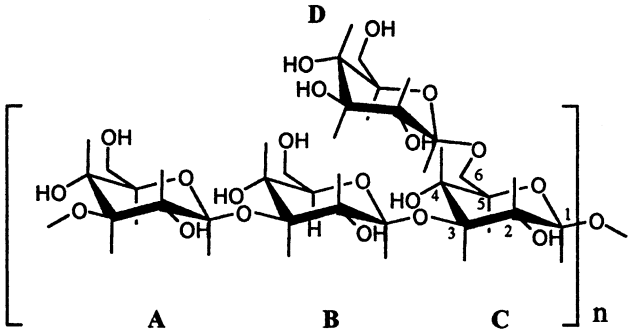


Scleroglucan

## 2. Experimental section

### 2.1. Materials

Scleroglucan of a nominal molecular weight of 157,000 was purchased from Sanofi Bio-Industries (France). Deuterated dimethylsulfoxide (DMSO-$d_6$) was purchased from Aldrich.

### 2.2. NMR relaxation experiments

$^{13}C$ NMR relaxation measurements were conducted at three $^{13}C$ Larmor frequencies, 75.4, 100.5 and 125.7 MHz on Bruker AC300, AM400, and AMX500 spectrometers, respectively, under broadband proton decoupling. The temperature was controlled to within $\pm1$°C by means of pre-calibrated thermocouples in the probe inserts. Spin–lattice relaxation times ($T_1$) were measured by the standard IRFT method with a repetition time longer than $5\times T_1$. A total of 256–720 transients were accumulated, for a set of 8–12 arrayed $t$ values, depending on the type of spectrometer and temperature. The 180° pulse width was ranged from 27 to 29 μs in the three spectrometers. Values of $T_1$ were determined by a three-parameter nonlinear procedure with a r.m.s. error of $\pm10\%$, or better. The reproducibility of each $T_1$ value was $\pm10\%$ or better. NOE experiments were carried out by the inverse gated decoupling technique. At least three experiments have been performed at each temperature value. Delays of at least 10 times the longest $T_1$ were used between 90° pulses. NOE values were estimated to be accurate to within $\pm15\%$.

Undegassed samples of scleroglucan in DMSO-$d_6$ solutions (3% w/v) were used for the $^{13}C$ relaxation experiments. Measurements with degassed samples did not show any measurable difference in the $^{13}C$ relaxation parameters relative to those of the undegassed samples in agreement with earlier reports (Dais, 1995; Tylianakis, Spyros, Dais, Taravel & Perico, 1999) in polysaccharide systems that show relaxation parameters in the milliseconds time-scale.

### 2.3. 2D NMR experiments

All 2D NMR experiments were conducted on a Bruker AMX500 spectrometer equipped with z-shielded gradient coils and an inverse multinuclear gradient probe-head and processed on a Silicon Graphics Indy workstation using the XWIN-NMR software (Bruker). Some details of the 2D NMR experiments used in the present study are given below (for a review of gradient COSY, TOCSY, gradient HMQC, and phase-sensitive NOESY experiments, see Braun, Kalinowski & Berger, 1996).

All 2D NMR spectra of scleroglucan in DMSO-$d_6$ solution were obtained at various temperatures from 303 to 383 K on the 500 MHz spectrometer. Due to the fast exchange of the hydroxyl protons at high temperatures, the corresponding signals were sufficiently broadened to eliminate overlaps with the signals of the ring protons. In addition, at high temperatures, the water peak shifts at higher fields, and does not interfere with the scleroglucan signals. Therefore, spectra at 283 K will be shown and discussed in the present study.

### 2.4. gCOSY

The gradient-selected H, H-COSY spectra for scleroglucan were recorded using 0.01 T/m sinusoidal shaped field gradients in 1:1 strength ratio with 2048 data points in the acquisition domain, 256 data points in $t_1$ and an increment of 198 μs for the $t_1$ evolution with 64 transients for each free induction decay, and a recycle delay of 1.5 s. Before Fourier transformation the data set in the $t_1$ dimension was zero-filled to 1024. Unshifted sinebell weighting functions were used in both dimensions.

### 2.5. TOCSY

The TOCSY spectra were measured in the phase-sensitive mode (TPPI) using MLEV-17 composite pulse cycle (Bax & Davis, 1985) and pre-irradiation of the water resonance. 2048 data points were used in the acquisition domain, 256 data points in $t_1$ and an increment of 142 μs for the $t_1$ evolution. 64 transients were acquired for each free induction decay, and a recycle delay of 1.5 s. Various mixing times ranged from 20–150 ms were used. Before Fourier transformation the data set in the $t_1$ dimension was zero-filled to 1024, and weighted with a Gaussian function

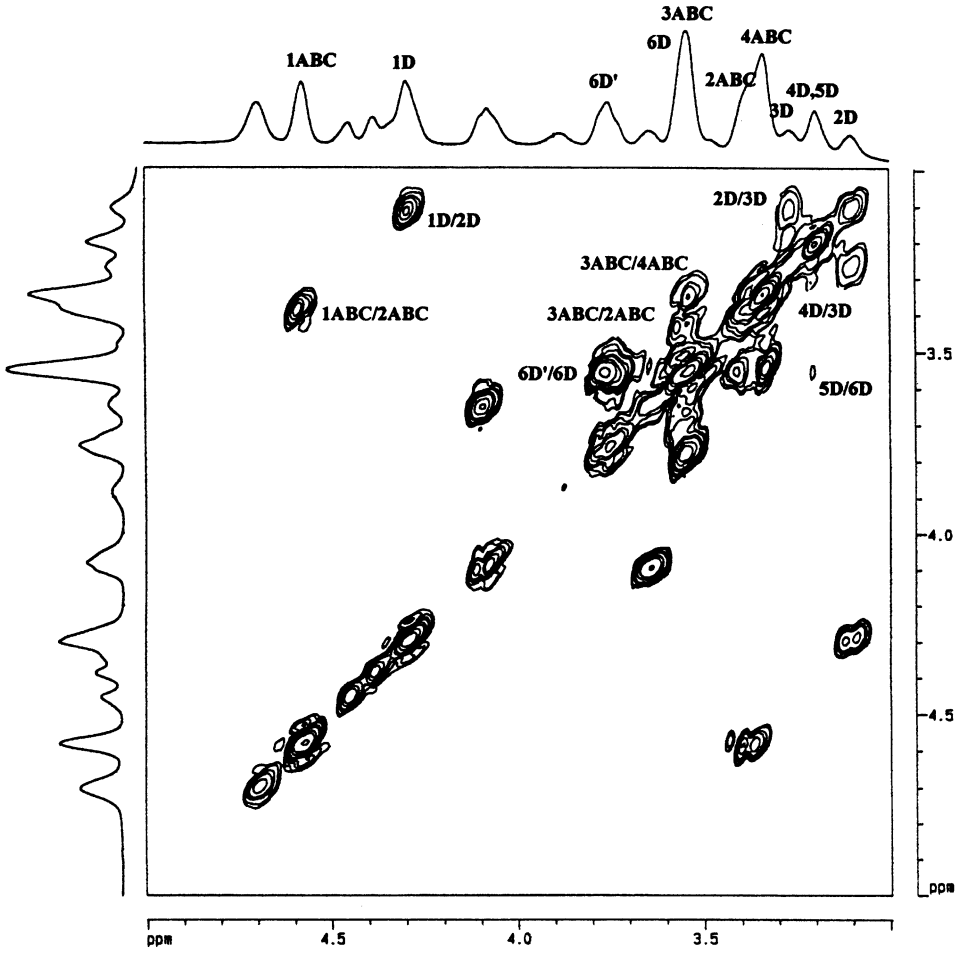


Fig. 1. 500 MHz gCOSY spectrum of scleroglucan at 283 K in dimethylsulfoxide-$d_6$.

in $t_2$ and $\pi/4$ shifted sinebell in $t_1$. The spectra were baseline corrected by a polynomial function.

### 2.6. NOESY

Phase-sensitive NOESY spectra with 2048 data points in the acquisition domain, 512 data points in $t_1$ and an increment of 110 μs for the $t_1$ evolution. 32 transients were acquired for each free induction decay with recycle delay of 2.0 s. Various mixing times ranged from 50–300 ms were used. Before Fourier transformation the data set in the $t_1$ dimension was zero-filled to 1024, and weighted with a Gaussian function in $t_2$ and a cosine window in $t_1$. The spectra were baseline corrected by a polynomial function.

### 2.7. gHMQC

The phase-sensitive gradient-selected hydrogen–carbon Heteronuclear Multiple Quantum Coherence experiments were performed with decoupling during acquisition using 0.01 T/m sinusoidal shaped field gradients in 5:3:4 strength ratio with 2048 data points in the acquisition domain, 256 data points in $t_1$ and an increment of 11.9 μs for the $t_1$ evolution with 32 transients for each free induction decay, and a recycle delay of 3.0 s. Before Fourier transformation the data set in the $t_1$ dimension was zero-filled to 1024, and processed with a four-fold forward linear prediction. The data set in the $t_1$ dimension was weighted with a squared sine window function, whereas that in the $t_2$ dimension was weighted with an exponential function.

### 2.8. Viscosity

Viscosity measurements were performed using Ubbelohde type dilution viscometers in a bath thermostatted at $30 \pm 0.01$°C. Intrinsic viscosities, $[\eta]$, and Huggins' constants, $k'$, were calculated through Eq. (1) by plotting reduced viscosity $\eta_{sp}/C$ vs. $C$.

$$\eta_{sp}/C = [\eta] + k'[\eta]^2 C \quad (1)$$

In this equation, $\eta_{sp}$ is the specific viscosity.

### 2.9. Numerical calculations

The relaxation data were analyzed by using the MOLDYN program (Craik, Kumar & Levy, 1983) modified by us to

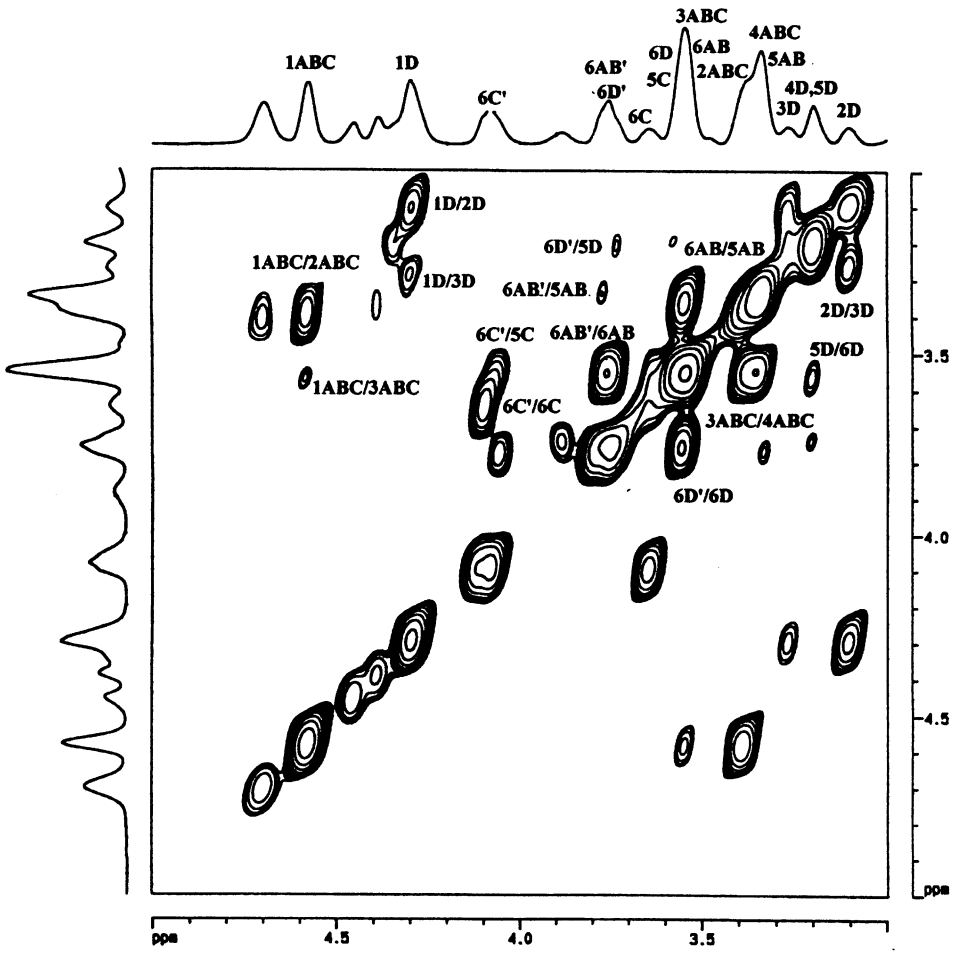


Fig. 2. 500 MHz TOCSY spectrum of scleroglucan at 283 K in dimethylsulfoxide-$d_6$.

include the spectral density functions used in the present study. Details of the program and fitting procedures by employing various models have been given elsewhere (Dais, 1987).

## 3. Results and discussion

### *3.1. $^{1}H$ and $^{13}C$ NMR spectra*

The gCOSY spectrum of scleroglycan in DMSO-$d_6$ solution at 283 K is shown in Fig. 1. The contour plot shows connectivities between the various protons within each D-glucopynosyl residue. However, even at 283 K severe overlaps of the various signals is observed. It is known that the signals of the anomeric protons of the $\beta(1 \rightarrow 3)$ linked D-glycopyranosyl residues appear at lower fields than those of the $\beta(1 \rightarrow 6)$ linked D-glycopyranosyl residues (De Bruyn, Anteunis & Verhegge, 1975). Therefore, the signal at $\delta$ 4.58 is assigned to the overlapped signal of the anomeric protons H-1ABC of glucopyranosyl residues A, B, and C in the backbone of the polymer (see structure **1**), whereas that at $\delta$ 4.32 is assigned to the anomeric protons H-1D of ring D. Following the cross-peaks pattern in the spectrum, protons H-2D and H-3D are unambiguously assigned. Proton H-3D is correlated with the signal at $\delta$ 3.21, which is attributed to the overlapped signals of protons H-4D and H-5D. The signals at $\delta$ 3.85 and 3.67 are assigned to the two diastereotopic protons H-6D and H-6′D of ring D following the cross-peak with the H-5D proton, and the cross-peak that connects the diastereotopic protons. Nevertheless, the signals of protons H-6D and H-6′D are overlapped by the proton signals of the other three rings. The signal at $\delta$ 3.40 is assigned to the overlapped signal of protons H-2ABC, since this signal is correlated with the H-1ABC signal. Following the cross-peaks in the spectrum signals H-3ABC and H-4ABC can be assigned. Also, the spectrum shows a cross-peak between signals at $\delta$ 4.09 and 3.63, the identity of which cannot be confirmed from this spectrum alone.

Support for this assignment of the proton spectrum is offered by the TOCSY experiment, which reveals remote signal connectivities by employing a spin-locking pulse. In this experiment, cross-peaks are observed between spins *k* and *m*, which are not directly coupled but share a mutual coupling partner 1, or between spins that are *J*-coupled with

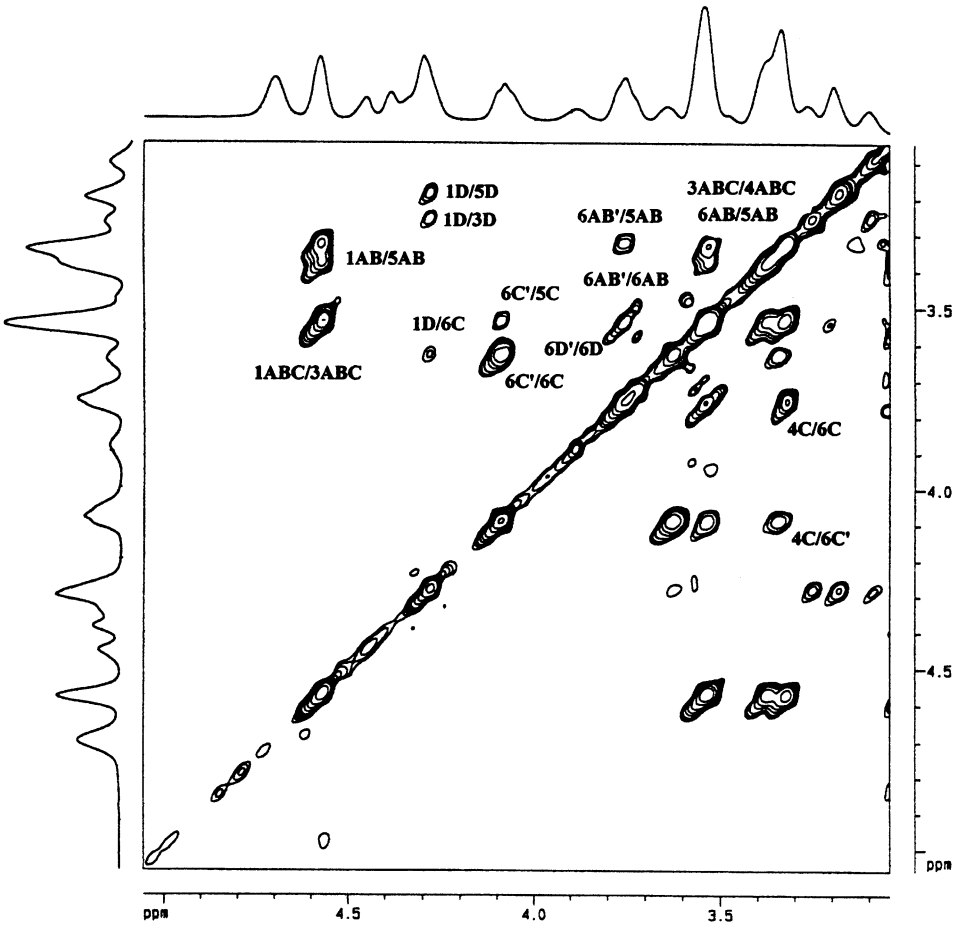


Fig. 3. 500 MHz NOESY spectrum of scleroglucan at 283 K in dimethylsulfoxide-$d_6$.

a magnitude less than the line widths of the individual resonances. Using spin-lock length of 20 ms, the TOCSY contour plot in Fig. 2 shows several remote connectivities. The connectivity pattern of protons H-1ABC and H-3ABC and that of protons H-1D and H-3D verify the correct assignment of protons H-3ABC and H-3D. Additional cross-peaks in the TOCSY spectrum reveal the overlapped signals of protons H-5AB, H-6AB, and H-6′AB. The identity of the peaks at $\delta$ 4.09 and 3.63 is resolved in this spectrum. They correspond to the H-6C and H-6′C protons, since the latter proton shows cross-peak with proton H-5C.

It should be noted that additional TOCSY experiments with longer mixing times have been performed in the course of this study in an attempt to detect connectivities through smaller coupling constants. None of these spectra gave a better connectivity around each ring than that observed in the TOCSY spectrum of Fig. 2.

The phase-sensitive NOESY experiment is expected to be more revealing than the previous homo-nuclear experiments because of its ability to correlate proton signals through dipole–dipole interactions in space. Indeed, the NOESY spectrum of scleroglucan in Fig. 3 obtained with mixing time of 300 ms shows a number of remote connectivities, such as H-1D, H-3D; H-1D, H-5D; H-1AB, H-5AB; H-4C, H-6C; H-4C, H-6′C; H-5C, H-6′C, and others shown in the spectrum that verify previous assignments. Apart from remote connectivities between protons in the same glucopyranosyl residues, the NOESY experiments could reveal connectivities between protons of neighboring glucopyranosyl residues provided that the dipole–dipole interactions between interesidue protons are effective. This method has been used in the past for the determination of the sequencing of the monosaccharide units in the polysaccharide chain (Scarsdale, Prestegard, Ando, Hori & Yu, 1986). In the contour plot of Fig. 3 a clear correlation between the H-1 proton of ring D and the proton H-6 of ring C is observed. Correlations between other interesidue protons are not clear due to severe overlaps.

The assignment of the $^{13}C$ NMR spectrum of scleroglucan has been attempted through a phase-sensitive gradient-selected Heteronuclear Multiple Quantum Coherence (gHMQC) experiment, which detects one-bond $^{13}C-^{1}H$ connectivities. The gHMQC spectrum of scleroglucan is shown in Fig. 4. This spectrum obtained with a delay time $\tau = 3.52$ ms ($^{1}J_{C,H} = 142$ Hz). Unfortunately, due to severe signal overlaps in the proton spectrum at 500 MHz, a few carbon signals can be assigned unambiguously. These are for carbons C-1D to C-5D for ring D, and carbons C-5C and

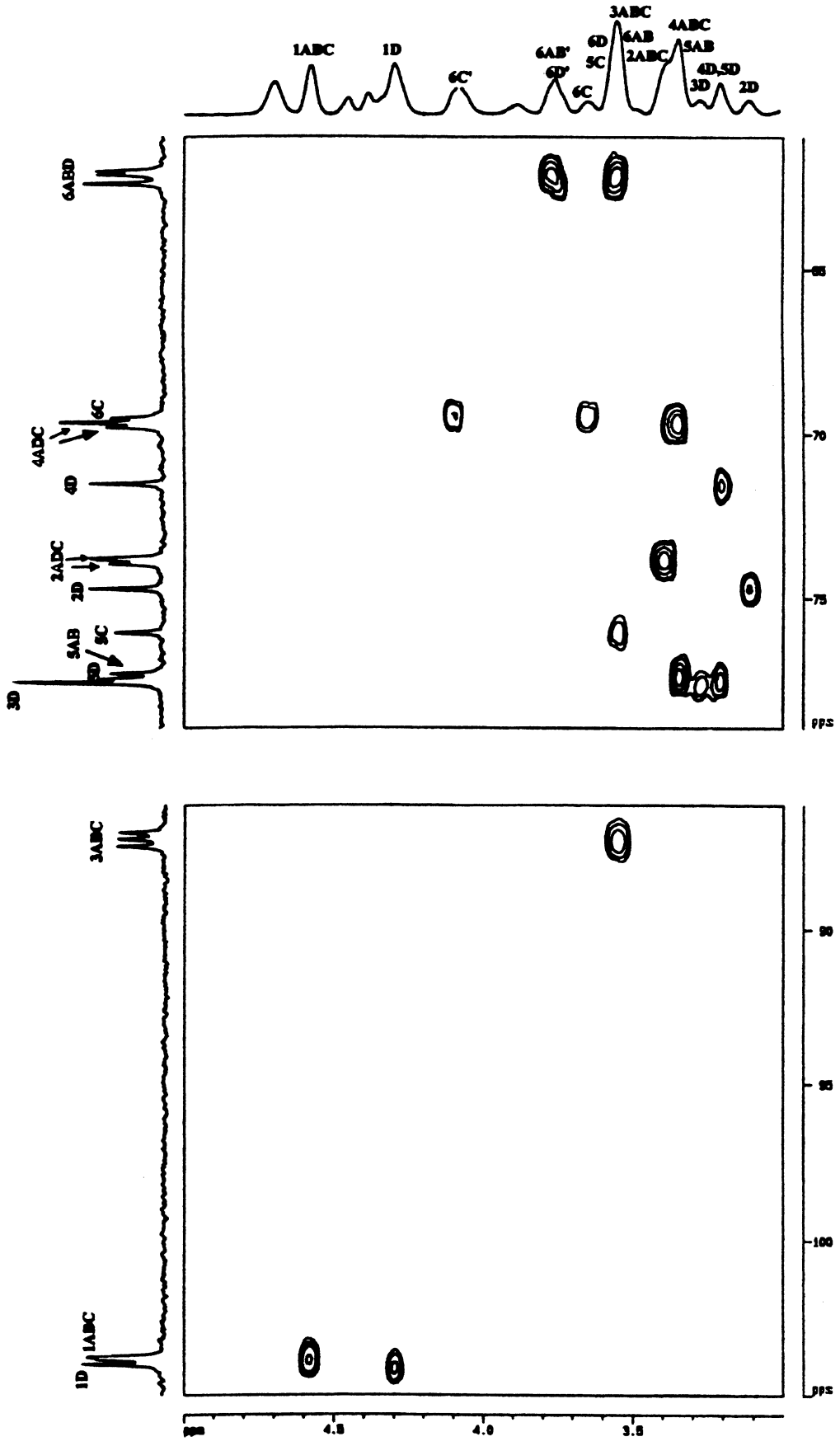


Fig. 4. 500 MHz gHMQC spectrum of scleroglucan at 283 K in dimethylsulfoxide-$d_6$. The spectrum has been expanded into two spectral regions for better observation of the various signals.

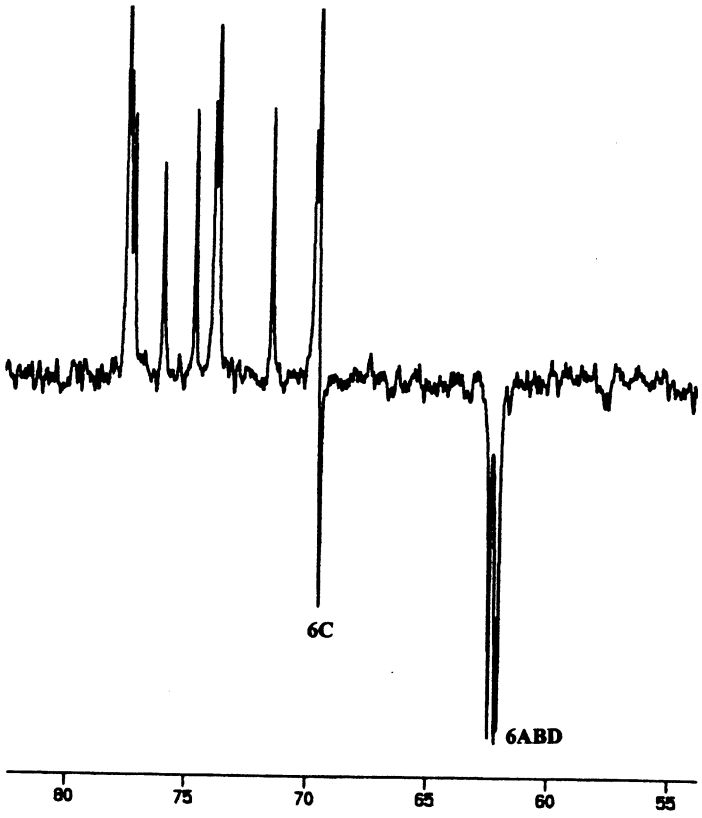


Fig. 5. Portion of the 500 MHz DEPT-135 spectrum of scleroglucan at 283 K in dimethylsulfoxide-$d_6$. Only the C-6 signals are inverted.

C-6C. The assignment of carbon C-6C, which appears at the lowest fields amongst the hydroxymethyl carbons, has been verified by performing the polarization transfer experiment DEPT-135 (Doddrell, Pegg & Bendall, 1982), which differentiates the CH and $CH_2$ carbon signals in the spectrum. The inclusion of a pulse angle $\Theta_{y'} = 135°$ in the pulse sequence of the experiment inverts only the carbon nuclei bearing two protons, whereas the CH ring carbons appear in the normal upright position. The DEPT-135 spectrum of scleroglucan is shown in Fig. 5. Also, the DEPT spectrum shows that the three signals at the highest fields, i.e. at $\delta$ 62.22, 62.00, and 61.88, belong to the hydroxymethyl carbons of rings A, B, and D. As we shall see later, these carbons can be assigned through relaxation measurements. The three signals at $\delta$ 87.45, 87.22, and 87.00 are not resolved in the gHMQC spectrum. However, they show a cross-peak with the overlapped peak H-3ABC of the proton spectrum and should correspond to the C-3A, C-3B, and C-3C carbons.

### 3.2. $^{13}C$ NMR relaxation data

Although the relaxation parameters $T_1$ and NOE of all resolved carbon resonances in the spectrum have been measured as a function of temperature and magnetic field, the present analysis will be restricted to the relaxation data of a few carbon resonances mainly for two reasons. The first is the incomplete assignment of the $^{13}C$ spectrum as discussed above. The second reason is the observation that the chemical shifts of the scleroglucan carbon resonances are strongly affected by temperature. Therefore, fewer carbon resonances are resolved in the spectra at lower temperatures than at high temperatures even at 125.7 MHz. For instance, 15 signals are resolved at 303 and 313 K, 16 at 333 K, 18 at 353 K, 20 at 373 K, and 22 at 383 K at 125.7 MHz. Moreover, the resolution was found to be dependent on the strength of the magnetic field as expected. What we need for the basic analysis of the dynamics of scleroglucan is the relaxation data of at least one-endocyclic carbon for each of the four rings. We will use the relaxation data of carbon C-5C of ring C at $\delta$ 75.87 and the resolved resonances for carbons of ring D. For the two rings A and B, the relaxation data of two of the three resolved resonances at $\delta$ 87.45, 87.22, and 87.00 will be used. The behavior of the experimental relaxation parameters $NT_1$ and NOE for the four carbons (C-5C, $\delta$ 87.45, 87.22 and 87.00) of the backbone residues with respect to temperature and magnetic field is shown in Fig. 6a–h.

The experimental relaxation data in Fig. 6 show a number of characteristics commonly observed in the $^{13}C$ relaxation data of most polymeric materials (Dais & Spyros, 1995; Tylianakis et al., 1999). (1) As temperature decreases, the $NT_1$ values ($N$ is the number of the directly attached protons) decrease monotonically, in all fields, reaching a minimum, which is followed by an increase in $NT_1$ with further

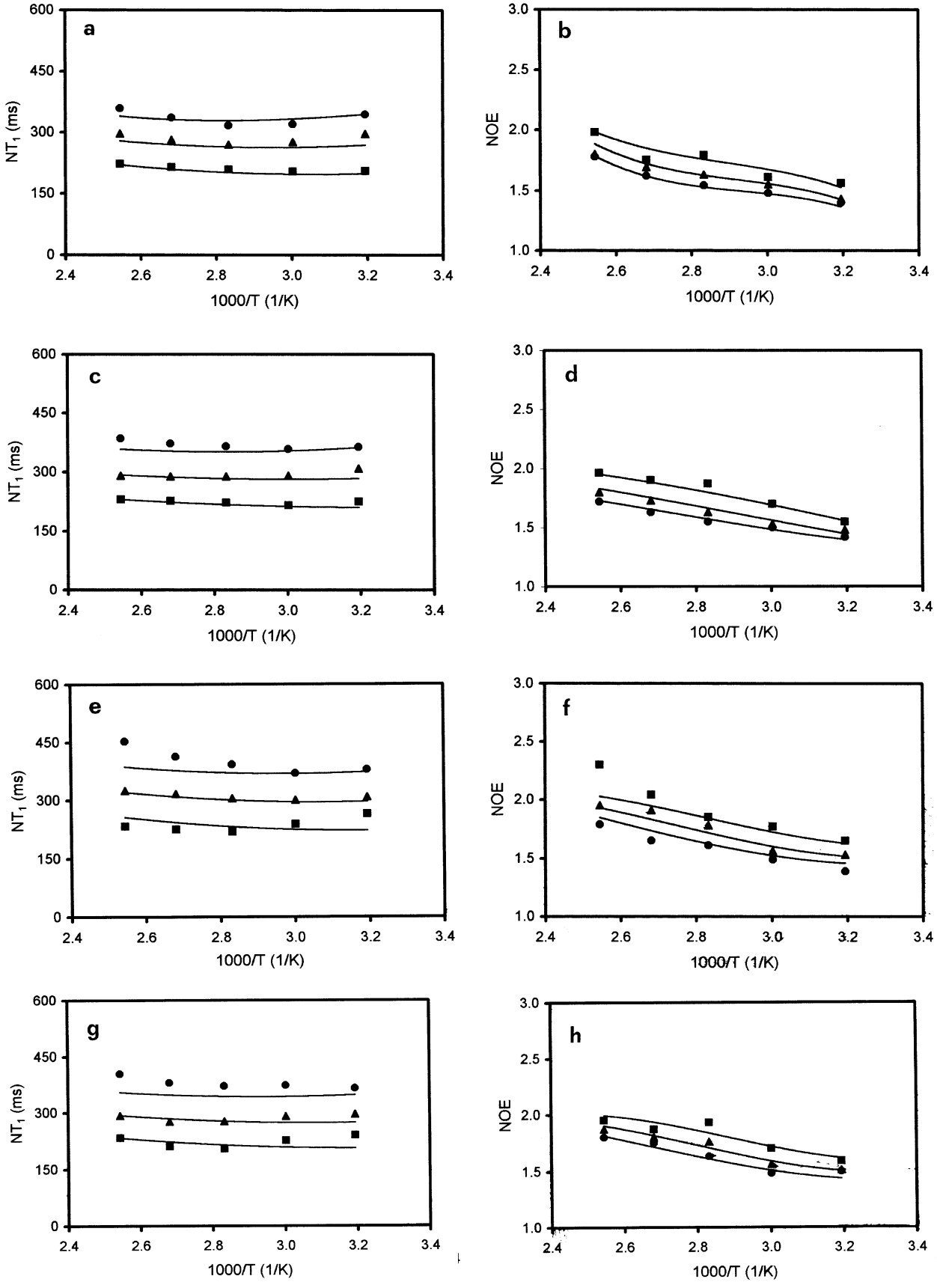
a
b
c
d
e
f
g
h
NT1 (ms)
NOE
1000/T (1/K)
600
450
300
150
0
3.0
2.5
2.0
1.5
1.0
2.4
2.6
2.8
3.0
3.2
3.4

Table 1
Simulation parameters of the DLM model used to describe backbone segmental motions of scleroglucan in dimethylsulfoxide-$d_6$ solutions

| | $\tau_1$(C-5C) (ns) | $\tau_1$(C-3C) (ns) | $\tau_1$(C-3A)[a,b] (ns) | $\tau_1$(C-3B)[b,c] (ns) |
|---|---|---|---|---|
| *Temperature (K)* | | | | |
| 313 | 1.55 | 1.47 | 1.27 | 1.28 |
| 333 | 1.13 | 1.09 | 1.07 | 1.03 |
| 353 | 0.87 | 0.83 | 0.72 | 0.77 |
| 373 | 0.78 | 0.72 | 0.65 | 0.61 |
| 393 | 0.51 | 0.56 | 0.49 | 0.46 |
| $\tau_0/\tau_1$ | 20 | 20 | 20 | 20 |
| $\tau_1/\tau_2$ | 100 | 100 | 75 | 75 |
| $\theta$ | 24 | 27 | 27 | 28 |
| $E_a$ (kJ mol$^{-1}$) | 13 | 12 | 12 | 13 |
| $r$ | 0.98 | 0.99 | 0.99 | 0.99 |

[a] Signal at $\delta$ 87.22.
[b] These values can be interchanged.
[c] Signal at $\delta$ 87.00.

decrease in temperature. This demonstrates that these carbons experience motions, which are within the "slow motional regime". (2) The minimum is shifted to higher temperatures (shorter correlation times) as the magnetic field increases. (3) At a given temperature, $NT_1$ values increase with increasing magnetic field. (4) The NOE values decrease with increasing magnetic field, although they tend to converge as temperature decreases reaching the slow motion regime. (5) Both $NT_1$ and NOE transitions are much broader than for small molecules. (6) At high temperatures, where motion becomes faster, NOE values are less than the theoretical maximum. These experimental observations preclude the possibility of describing the scleroglucan local dynamics by using a single-exponential correlation function.

### 3.3. Dynamic modeling of scleroglucan

In modeling the dynamics of polysaccharides two types of motions are considered (Tylianakis et al., 1999): First the overall rotatory diffusion of the carbohydrate chain as a whole and second, local chain motions. Local chain motions in a carbohydrate chain are considered to be: (1) the oscillatory motions about the D-glycosidic bonds, which represent the so-called segmental motions; (2) internal motions of substituents attached to the carbohydrate chain via chemical bonds, such as the hydroxymethyl groups. (3) A third type of very fast local motions (about $10^{-11}$ s), which have been found to occur in other polysaccharide systems (Tylianakis et al., 1999), are the small amplitude librations of particular backbone C–H vectors within a potential well. Each of these motions is considered to be an independent source of motional modulation of the $^{13}C-^{1}H$ dipole–dipole interactions for the protonated carbons of the polysaccharides.

### 3.4. Overall rotatory diffusion

For sufficiently high molecular weight random coil polymers (above a critical value of 1000 to 10,000 depending on chemical structure), the overall motion is much slower than the chain local motions. Thus, it makes a negligible contribution to the $T_1$ values of the backbone and side-chain carbons (Dais & Spyros, 1995; Heatley, 1979). The molecular weight of the present polysaccharide molecule lies above this limit. Our neglect of the overall motion is further supported by estimation of the overall motion correlation time, $\tau_R$ of scleroglucan. Since the correlation time of the overall motion cannot be determined from relaxation data alone (all carbons in the carbohydrate chain relax via both the overall and local motions), this parameter must be simulated by using the hydrodynamic Eq. (2) (Isihara, 1968).

$$\tau_R = \frac{2M_W[\eta]\eta_o}{3RT} \quad (2)$$

$M_w$ is the molecular weight; $[\eta]$ the intrinsic viscosity of the polymer solution; $\eta_o$ the solvent viscosity. By substituting in Eq. (2) the measured intrinsic viscosity of scleroglucan solution, $[\eta] = 3.15$ dl dg$^{-1}$, its molecular weight, $M_w = 157,000$ g mol$^{-1}$, and the viscosity of dimethylsulfoxide at 30°C, 1.808 cP, we obtain the correlation time for the overall motion, $\tau_R = 2.35 \times 10^{-5}$ s. The calculated $\tau_R$ for scleroglucan should represent the polysaccharide behavior in the high molecular weight limit. The reported relaxation

Fig. 6. Temperature dependence of the experimental relaxation data for the ring carbons of scleroglucan in dimethylsulfoxide-$d_6$ solutions at magnetic fields (■) 75.4; (▲) 100.5; and (●) 125.7 MHz. For carbon C-5C (a) $NT_1$, (b) NOE; for carbon signal at $\delta$ 87.45 (c) $NT_1$, (d) NOE; for carbon signal at $\delta$ 87.22 (e) $NT_1$, (f) NOE; for carbon at $\delta$ 87.00 (g) $NT_1$, (h) NOE. Solid curves correspond to the DLM model fitting of $NT_1$ and NOE values.

Table 2
$^{13}C$ spin–lattice relaxation times ($NT_1$, in ms) and NOE values (in parentheses) of the hydroxymethyl carbons of scleroglucan as a function of temperature and magnetic field

| Temperature (K) | Magnetic field (MHz) | | | | | | | | |
|---|---|---|---|---|---|---|---|---|---|
| | C-6A[a,b] | | | C-6B[b,c] | | | C-6D | | |
| | 75.4 | 100.5 | 127.9 | 75.4 | 100.5 | 127.9 | 75.4 | 100.5 | 127.9 |
| 333 | 224 (1.93) | 336 (1.83) | 376 (1.67) | 262 (2.05) | 350 (1.82) | 364 (1.77) | 356 (2.05) | 384 (2.00) | 410 (1.79) |
| 353 | 302 (2.05) | 378 (2.00) | 464 (1.84) | 318 (2.06) | 387 (1.90) | 458 (1.77) | 428 (2.22) | 490 (2.18) | 544 (2.14) |
| 373 | 346 (2.15) | 418 (2.02) | 516 (1.90) | 358 (2.16) | 420 (2.07) | 560 (1.95) | 564 (2.30) | 606 (2.24) | 764 (2.22) |
| 393 | 420 (2.22) | 466 (2.16) | 592 (2.07) | 430 (2.24) | 470 (2.23) | 598 (2.15) | 760 (2.38) | 822 (2.31) | 944 (2.30) |

[a] Signal at $\delta$ 62.00.
[b] These values can be interchanged.
[c] Signal at $\delta$ 61.88.

parameters are therefore dominated by local polymer dynamics.

### 3.5. Segmental motions

In polymers, the dominant relaxation process is the $^{13}C-^{1}H$ dipolar interactions. Also, for these systems, only interactions with directly bonded protons need be considered. Under conditions of complete proton decoupling the $^{13}C$ relaxation parameters, $NT_1$ and NOE can be written in terms of the spectral density function, $J_i(\omega_i)$, as follows (in the SI system) (Doddrell, Glushko & Allerhand, 1972):

$$\frac{1}{NT_1^{DD}} = \frac{\Omega}{10}[J_0(\omega_H - \omega_C) + 3J_1(\omega_C) + 6J_2(\omega_H + \omega_C)] \tag{3}$$

$$\mathrm{NOE} = 1 + \frac{\gamma_H}{\gamma_C} - \frac{\Omega T_1}{10}[6J_2(\omega_H + \omega_C) - J_0(\omega_H - \omega_C)] \tag{4}$$

and

$$\Omega = \left(\frac{\mu_0 \gamma_H \gamma_C h}{8\pi^2 r_{CH}^3}\right)^2$$

Where, $\gamma_H$ and $\gamma_C$ are the gyromagnetic ratios of proton and carbon nuclei, respectively; $\omega_H$ and $\omega_C$ their Larmor frequencies; $\mu_0$ the vacuum magnetic permeability; h the Planck's constant; $N$ the number of directly bonded protons; $r_{CH}$ the C–H internuclear distance.

The spectral density function required for the calculation of the relaxation parameters by means of Eqs. (3) and (4) should be obtained upon Fourier transform of the appropriate time-correlation function,

$$J_m(t) = 2\mathrm{Re}\left[\int_0^\infty G_m(\omega)\, e^{i\omega t}\, dt\right] \tag{5}$$

with Re indicating the real part of the complex Fourier transform.

Several attempts (Catoire, Derouet, Redon, Goldberg & Herve du Penhoat, 1997; Dais, 1987, 1995; Dais & Marchessault, 1991; Tylianakis, Dais, Andre & Taravel, 1995; Tylianakis et al., 1999) have been made in the past to interpret the relaxation behavior of polysaccharides in solution by employing a variety of theoretical TCFs (models). The ability of the various models to describe the dynamics of the segmental motions of polysaccharides in solutions has been tested in previous publications on linear homo-polysaccharides (Dais, 1987, 1995; Tylianakis et al., 1995, 1999). Amongst these, the bimodal time-correlation function developed by Dejean, Lauprêtre, and Monnerie (DLM) (Dejean de la Batie, Lauprêtre & Monnerie, 1988) offered a much better description of the segmental dynamics of these biopolymers. Therefore, the DLM model will be used in the following analysis.

The DLM time-correlation function describes the backbone reorientation in terms of two motional processes. (1) A diffusion process along the carbohydrate chain, which occurs via conformational transitions described by two correlation times $\tau_0$ and $\tau_1$, for isolated conformational transitions and for cooperative transitions, respectively, and (2) bond librations, i.e. wobbling in a cone motion of the backbone internuclear C–H vectors. The librational motion is associated with a correlation time $\tau_2$, whereas the cone half-angle $\theta$ determines the extent of the libration about the rest position of the C–H bond that coincides with the axis of the cone. The DLM spectral density function is given explicitly by Dejean de la Batie et al., 1988.

The best fit $NT_1$ and NOE data, as a function of temperature and magnetic field for the four backbone ring carbons of the repetitive unit of scleroglucan by employing the DLM model is shown graphically in Fig. 6a–h. It is seen from these plots that good agreement between experimental and calculated values is obtained from this model throughout the entire temperature range studied. In all cases, the percent difference between the experimental and calculated values was within the experimental error ($\pm 10\%$ for $T_1$ and $\pm 15\%$ for the NOE values) of the relaxation measurements. For this model, the values of the fitting parameters are summarized in Table 1.

Table 3
$^{13}$C spin–lattice relaxation times ($NT_1$, in ms) and NOE values (in parentheses) of the five-endocyclic carbons of ring D of scleroglucan as a function of temperature and magnetic field

| Temperature (K) | Magnetic field (MHz) | | | | | | | | | |
|---|---|---|---|---|---|---|---|---|---|---|
| | C-2D | | | C-3D | | | C-4D | | | C-5D | | |
| | 75.4 | 100.5 | 125.7 | 75.4 | 100.5 | 125.7 | 75.4 | 100.5 | 125.7 | 75.4 | 100.5 | 125.7 |
| 313 | 259 (1.81) | 317 (1.67) | 363 (1.65) | 260 (1.75) | 354 (1.66) | 393 (1.62) | 263 (1.70) | 320 (1.65) | 380 (1.54) | 264 (1.74) | 328 (1.62) | 361 (1.65) |
| 333 | 258 (1.91) | 327 (1.76) | 390 (1.70) | 266 (1.85) | 338 (1.71) | 395 (1.74) | 286 (1.93) | 360 (1.81) | 390 (1.74) | 285 (1.83) | 351 (1.82) | 385 (1.74) |
| 353 | 293 (2.03) | 385 (1.95) | 450 (1.86) | 282 (1.88) | 363 (1.86) | 450 (1.84) | 306 (2.00) | 361 (1.96) | 458 (1.86) | 304 (1.96) | 391 (2.06) | 431 (2.00) |
| 373 | 358 (2.23) | 414 (2.06) | 535 (2.00) | 343 (2.24) | 425 (2.08) | 524 (1.95) | 388 (2.31) | 407 (2.08) | 508 (2.11) | 374 (2.35) | 444 (2.20) | 543 (2.06) |
| 393 | 415 (2.50) | 544 (2.32) | 644 (2.11) | 431 (2.47) | 541 (2.15) | 655 (2.05) | 424 (2.39) | 528 (2.32) | 675 (2.20) | 451 (2.43) | 551 (2.32) | 650 (2.22) |

Comparison of the motional parameters in Table 1 leads to the following conclusions: First, the $\tau_1$ values for carbon C-5C are similar to those of carbon at $\delta$ 87.45 at all temperatures. This similarity indicates that the signal at $\delta$ 87.45 belongs to carbon C-3C. Second, The $\tau_1$ values for carbon C-5C (and C-3C) are larger than the $\tau_1$ values of carbons at $\delta$ 87.22 and 87.00 at all temperatures. This observation indicates that the segmental motion of residue C is slower than that of the other two backbone residues. This provides direct evidence of the smaller flexibility of the scleroglucan chain at the junction point. Third, no significant differences in the $\tau_1$ parameters of carbons at $\delta$ 87.22 and 87.00 are observed. This indicates that rings A and B are characterized by the same flexibility. Residues A and B are placed between two junction points of the chain, and are expected to show the same relative flexibility.

Plots of the logarithms of these values as a function of $1/T$ (K) show linear correlations, in the temperature range studied, yielding apparent activation energies, $E_a$ (in kJ mol$^{-1}$) for the various carbon sites. These values are summarized in Table 1, along with the correlation coefficients of the Arrhenius fit.

Besides the correlation times describing backbone motions, the angle $\theta$ of the librational motions plays an important role in determining the nature of local dynamics. This angle has been related to the steric hindrance exerted on the C–H bond librational motion at the considered site: the larger the steric hindrance, the smaller is $\theta$. The simulated values for the angles $\theta$ of the C–H vectors at carbon sites C-3A, C-3B, and C-3C are not very different, indicating the same local dynamics at these carbon sites. However, the angle $\theta$ for carbon C-5C is smaller than that for carbon C-3C of the same ring (Table 1). This difference in the $\theta$ values reflects the different magnitude of the steric hindrance to the librational motion at the C-3C and C-5C carbon sites of scleroglucan. An explanation for the observed difference in the librational angle at position C-5C of scleroglucan relative to that at the C-3C carbon could be the presence of hydroxymethyl group, which hinders the librational motions of the C-5–H-5 vectors.

### 3.6. Internal motions

There are two kinds of internal motions occurring in scleroglucan. Simple internal rotations of the free hydroxymethyl groups of the backbone rings A and B about the exocyclic C-5–C-6 bonds, and multiple internal rotations involving the exocyclic hydroxymethyl groups of rings C and D, as well as the ring D itself. However, to describe quantitatively internal rotations in the scleroglucan molecule, we need to know first the assignment of the signals for the various hydroxymethyl carbons in the $^{13}$C NMR spectrum. The signal of the C-6C carbons has been assigned previously through gHMQC spectrum and the 1D DEPT-135 experiment at 283 K. Amongst the signals in the region where the free hydroxymethyl carbons appear, the signal at

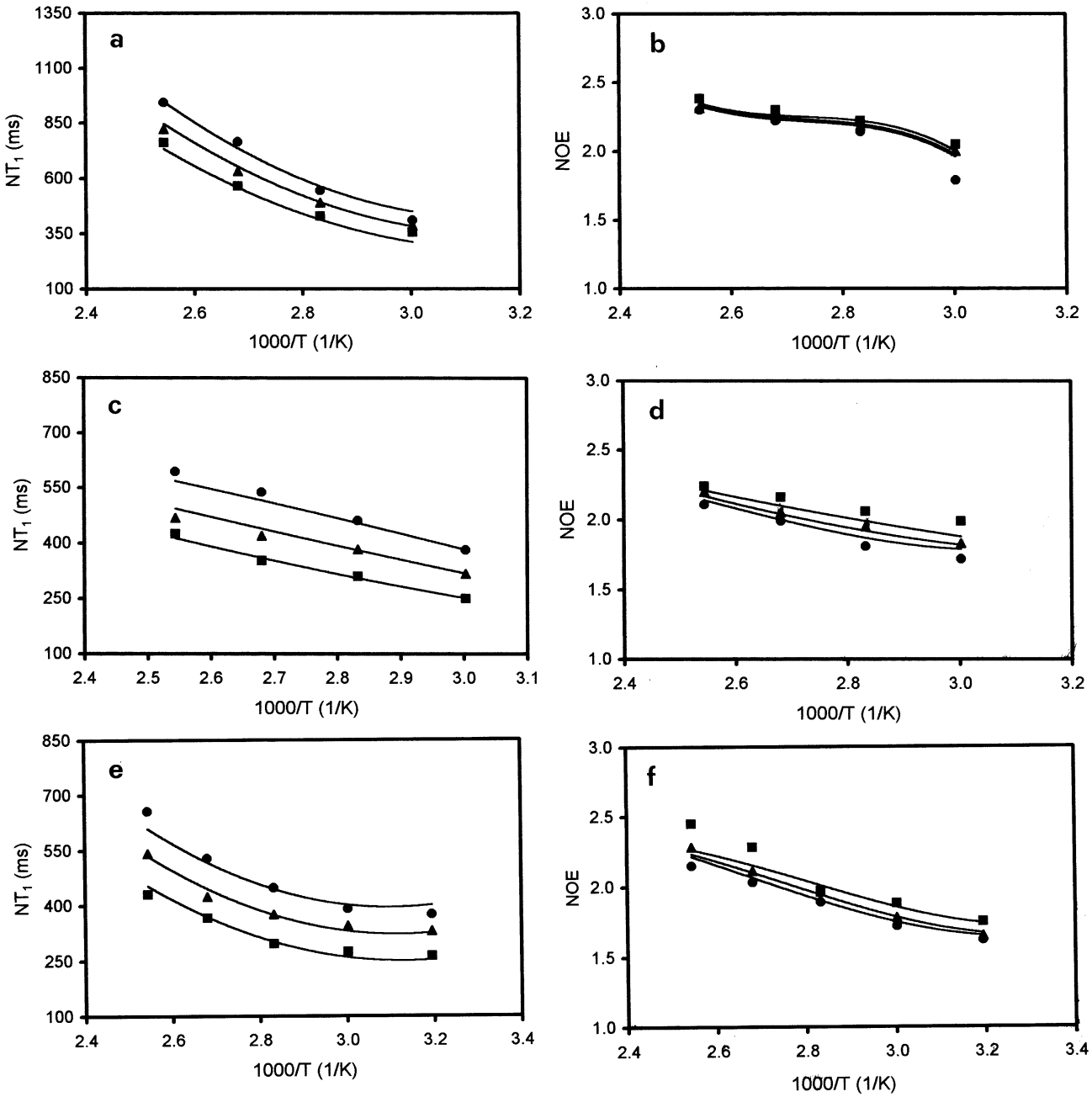


Fig. 7. Temperature dependence of the experimental relaxation data for the hydroxymethyl carbons of scleroglucan in dimethylsulfoxide-$d_6$ solutions at magnetic fields (■) 75.4, (▲) 100.5, and (●) 125.7 MHz. For carbon C-6D (a) $NT_1$, (b) NOE; for carbon signal at $\delta$ 62.00 and 61.88 (c) $NT_1$, (d) NOE; for the endocyclic carbons of ring D (e) $NT_1$, (f) NOE. Solid curves correspond to the DLM model fitting of $NT_1$ and NOE values.

$\delta$ 62.22 is characterized by the longest relaxation time at all temperatures. This signal is attributed to the C-6D carbon. This carbon being in the D-glucopyranosyl residue of the side chain of scleroglucan is relaxed via multiple internal rotations, and hence is expected to be more flexible than the other free hydroxymethyl moieties (Spyros, Dais & Heatley, 1994). The signals at $\delta$ 62.00 and 61.88 belong to the free hydroxymethyl carbons of rings A and B. However, these signal cannot be assigned on the basis of their relaxation parameters, since both their $NT_1$ and NOE values are similar within 5–10%. The similarity of the relaxation parameters for these carbons indicates that the rates of the hydroxymethyl group internal rotations in rings A and B are comparable within experimental error. Therefore, an average value of the relaxation parameters for these carbons is considered in the present analysis. For the same reason, an average value of the relaxation parameters at each temperature will be used for the endocyclic carbons of the D ring.

Table 4
Simulation parameters of the restricted diffusion model, and the restricted multiple internal rotations model used to describe side chain motions (hydroxymethyl groups and ring D) of scleroglucan in dimethylsulfoxide-$d_6$ solutions

| | $D_i$(C-6AB)[a] $\times 10^9$ | $2\chi$(AB)[a] | $D_i$(ring D)[b] $\times 10^9$ | $2\chi$(ring D)[b] | $D_i$(C-6D) $\times 10^9$ | $\chi$(C-6D) |
|---|---|---|---|---|---|---|
| *Temperature (K)* | | | | | | |
| 313 | | | 5.55 | 98 | | |
| 333 | 4.29 | 102 | 5.78 | 106 | 4.31 | 117 |
| 353 | 8.69 | 114 | 7.51 | 115 | 6.02 | 138 |
| 373 | 9.99 | 128 | 8.67 | 136 | 10.46 | 148 |
| 393 | 11.56 | 140 | 12.35 | 156 | 14.03 | 170 |
| $E_a$ (kJ mol$^{-1}$) | 17 | | 18 | | 22 | |
| $r$ | 0.95 | | 0.99 | | 0.99 | |

[a] Diffusion coefficients and amplitudes of restricted motions for both the hydroxymethyl groups of rings A and B.
[b] Diffusion coefficients and amplitudes of restricted motions for the endocyclic carbons of ring D.

The relaxation parameters of the three free hydroxymethyl carbons and the endocyclic carbons of ring D as a function of temperature and magnetic field are summarized in Tables 2 and 3. It is worth mentioning that Table 2 and 3 do not contain the relaxation parameters of the C-6C and C-1D carbons, respectively, since the corresponding signals in the $^{13}$C NMR spectrum are not resolved over the whole temperature range of the present relaxation measurements.

Fig. 7a–f depicts the variation of the $NT_1$ and NOE values for carbons C-6D, the average values for C-6A, C-6B, and the average values for the four-endocyclic carbons of the D ring. As can be seen from this Fig. 7, the $NT_1$ values for all the side chain carbons increase monotonically with increasing temperature, and thus fall within the "fast motion regime" in all three fields. At a given temperature and magnetic field, the average relaxation times of carbons C-6A and C-6B are higher than the values of the endocyclic carbons of rings A and B (compare Figs. 6e, g and 7c). This trend reflects the increasing flexibility of the hydroxymethyl groups owing to internal motions about the exocyclic bonds C-5–C-6.

The relaxation times of the side chain D ring carbons are higher than those of the C-5 and/or C-3 carbons of C ring at the junction point, and increase on going from the endocyclic ring carbons to the end C-6D hydroxymethyl carbon (compare Figs. 6a, c and 7c, e). This observation, which is more pronounced at higher temperature, is not surprising since these carbons relax via multiple internal rotations about the three bonds forming the (1 → 6)-D-glucosidic linkage, and the exocyclic bond C-5–C-6 for the C-6D carbon, as mentioned earlier. This trend, which has been observed in other polymer systems with long side chains (Dais & Spyros, 1995), reflect an increasing internal mobility of the side chain towards its free end, owing to internal rotations about successive C–C bonds.

The relaxation data of the side chains of scleroglucan were analyzed by employing appropriate theoretical time-correlation functions, which will be presented below. To facilitate this analysis we have made the following clarifications and assumptions. (1) The sole relaxation mechanism considered for the side chain groups is the $^{13}$C–$^{1}$H dipole–dipole interactions. (2) All internal motions of the side chains are considered to be independent from segmental motion. This assumption is valid when the time-scale of the side chain motions is at least two orders of magnitude higher than the time-scale of segmental motion, the former motion being in the extreme motional narrowing region. For comparable time-scales, this assumption is a first approximation. As we shall see later, this assumption holds for the present system. (3) All internal motions of the side chains are considered to be independent from each other. This assumption may be valid for short side chains and for free internal motions. However, for internal rotations of restricted amplitude, this assumption is valid only for relatively large angular amplitudes. (4) Individual bond rotations inside the β(1 → 6) glucosidic bridge cannot be treated quantitatively due to the lack of sufficient relaxation data. However, these rotations are effective in modulating local magnetic fields, and thus are expected to cause relaxation of the side chain D-glucopyranosyl carbons. The cumulative effect of rotations about the β(1 → 6) glucosidic bonds will be estimated by considering rotation of the D ring about the virtual bond connecting the C-5C and C-1D carbons.

A number of models exist in the literature describing internal mobility as a free rotation, restricted rotation about a bond, a wobbling motion in which a vector diffuses within a cone, or jumps between equivalent, or nonequivalent states. An extensive discussion of these models can be found in the references cited (Dais, 1987, 1995; Dais & Spyros, 1995). The internal motion of the hydroxymethyl groups of rings A and B about the exocyclic C-5–C-6 bonds superimposed on segmental motion cannot be described by assuming free rotation of 360° about this bond. Indeed, composite TCFs (Spyros & Dais, 1992) based on the DLM model and the Woessner equations (Woessner, 1962) for stochastic diffusion and jump processes did not reproduce the experimental data for the C-6A and C-6B carbon of scleroglucan. For this reason time-correlation

functions describing restricted internal motions superimposed on segmental motion should be used in the present analysis. Such TCFs are the internal two-state jump TCF (London, 1978), and the restricted-amplitude internal diffusion TCF (London & Avitabile, 1978). Both TCFs have been used previously to describe the hydroxymethyl internal motions of several linear homo-polysaccharides (Tylianakis et al., 1995, 1999). Only the diffusion model was successful in reproducing the experimental $NT_1$ and NOE data for A and B hydroxymethyl carbons of scleroglucan, and resulted in physically realistic values of the correlation times, which follow an Arrhenius-type behavior. In this model, O-6A and/or O-6B atoms moves continuously between two limiting values of an angle $\chi$ (i.e. the amplitude of restricted motion is $2\chi$). Restricted diffusion about a single axis has been solved analytically (London & Avitabile, 1978) and the resulting TCF can be combined with the TCF of the DLM model to give a new composite TCF, which incorporates the diffusion constant, $D_i$, associated with internal motion. The composite TCFs for both models can be found in reference cited (Dais & Marchessault, 1991).

Fig. 7c and d show the best fit to the average experimental $NT_1$ and NOE values of the C-6A and C-6B carbons obtained by using the restricted diffusion model. Clearly, the agreement between the experimental and calculated values is very good. Table 4 summarizes the optimized parameters of the diffusion model. The diffusion coefficients, $D_i$(AB), for the A and B hydroxymethyl internal rotation are about two orders of magnitude higher than the correlation times, $\tau_1$, of the segmental motion of rings A and B. The Arrhenius plots of the diffusion coefficients, $D_i$(AB) gave an apparent activation energy of 17 kJ mol$^{-1}$. Internal rotations are restricted in nature characterized by amplitudes between 100–140° in the temperature range of 60°C.

Composite TCFs and their Fourier transform pair, spectral density functions, for side chain motions superimposed on polymer segmental motions have been developed recently (Spyros & Dais, 1995a) in an attempt to describe multiple internal rotations of hydrocarbon side chains attached to polymer backbone (Spyros & Dais, 1995b). The composite spectral density for side chain restricted rotations superimposed on chain segmental motion, the latter being described by the DLM model, is given explicitly in reference cited (Spyros & Dais, 1995a). It involves the correlation times, $\tau_0$ and $\tau_1$, describing segmental motions, the diffusion constants, $D_i$, for rotation about the $i$th diffusion axis, and the angle, $2\chi_i$, which is the range of angular restriction. Apart from the experimental relaxation data, the model requires as input parameters the angles, $\beta_{ij}$, formed between successive internal rotation axes, and the angle, $\beta_{n\mathrm{F}}$, formed between the $n$th rotation axis and the last C–H bond. Also, the Euler angles, $\alpha_{ij}$, specifying the torsional angles between $C_{i-2}$–$C_{i-1}$ and $C_i$–$C_{i+1}$ bonds when viewed along the $C_{i+1}$–$C_i$ bond axis. This composite spectral density function will be used to describe multiple internal rotations of ring D about the virtual bond C-5C–C-1D and its hydroxymethyl group about the C-5D–C-6D bond.

The angles formed between the axis of rotation C-5C–C-1D and the five-endocyclic C–H bonds of ring D are estimated from the minimum energy structure of scleroglucan obtained by employing the program POLYS (Engelsen, Cros, Mackie & Perez, 1996). These are 122.6° for the C-1–H-1 vector, 122.5° for the C-2–H-2 vector, 125.7° for the C-3–H-3 vector, 118.0° for the C-4–H-4 vector, and 119.6° for the C-5–H-5 vector. The fact that all C–H bonds form nearly the same angles with the virtual bond C-5C–C-1D, and that the endocyclic carbons are characterized by similar relaxation parameters, supports our decision to use this bond as the axis of internal rotation. In the subsequent calculations an average value of 121.7° for this angle is used. The tetrahedral angle of 109.5° is used for the angle formed between the C-6–H-6 vectors and the internal axis C-5–C-6 of ring D, whereas a value of 76.7° is used for the angle $\beta$, formed between the two successive axes of rotation. The latter value is obtained from the minimum energy structure of scleroglucan.

The results of fitting the experimental data of the endocyclic carbons of ring D, and the C-6D carbons by using the model for multiple internal rotations are compiled in Table 4. This model was able to reproduce the experimental data of the side chain carbons over a temperature range of 60–70°C at three magnetic fields. The quality of the fit for the $NT_1$ and NOE data is shown in Figs. 7a, b, e and f. The two parameters $D_i$(ring D) and $2\chi_i$(C-6D) of the model give the rate of diffusion and the amplitude of the restricted motion about successive internal bonds of the side chain, respectively. Each $D_i$ value increases with temperature, and at a given temperature, $D_i$ generally increases on going from the ring towards the terminal exocyclic bond C-5–C-6. The rotation of the terminal hydroxymethyl group is faster as expected.

The diffusion constant for each bond rotation shows a linear dependence on temperature. Although there is a large error (~30%) in the calculated activation energies, these values are nearly constant along the side chain, and not different from the activation energies of the restricted rotation of the free hydroxymethyl groups of rings A and B (Table 4). The angular amplitude $2\chi_i$ for rotation about each successive bond of the side chain increase with temperature. This observation indicates a greater mobility of the side chain as temperature increases, in accord with the physical picture described by the model. The angular amplitude along the chain increases from the first to the terminal bond, where the angular constraints are expected to be more relaxed.

## 4. Conclusions

On the basis of the variable temperature $NT_1$ and NOE

measurements at three magnetic fields, the backbone and side chain motions of the branched polysaccharide scleroglucan were investigated by employing a number of dynamic models. Although difficulties in the assignment of the $^{13}C$ NMR spectrum of scleroglucan restrict the complete treatment of the relaxation data, the present results give an insight into the nature of segmental and side chain motions occurring in the complex branched polysaccharide.

The analysis of the $NT_1$ data of the resolved resonances of the protonated carbons of the backbone D-glycopyranosyl residues, and in particular, of the more sensitive to the local environment NOE values, employing the DLM model, demonstrates the importance of librational motions for describing local motions in the main chain. Regarding the side chain motions, internal rotations of limited amplitude superimposed on the backbone motion offer the best interpretation of the relaxation data of the exocyclic free hydroxymethyl groups, and the pendent D-glucorynasosyl ring.

## Acknowledgements

We gratefully acknowledge financial support from the French–Greek Scientific Committee for Research and Technology (Program PLATON).

## References

Bardet, M., Rousseau, A., & Vincendon, M. (1993). High-resolution solid-state $^{13}C$ CP/MAS study of scleroglucan hydration. *Magnetic Resonance in Chemistry*, *31*, 887–892.

Bax, A., & Davis, D. G. (1985). Practical aspects of two-dimensional transverse NOE spectroscopy. *Journal of Magnetic Resonance*, *63*, 207–213.

Bluhm, L. T., Deslandes, Y., Marchessault, R. H., Perez, S., & Rinaudo, M. (1982). Solid-state and solution conformation of scleroglucan. *Carbohydrate Research*, *100*, 117–130.

Bo, S., Milas, M., & Rinaudo, M. (1987). Behavior of scleroglucan in aqueous solution containing sodium hydroxide. *International Journal of Biological Macromololecules*, *9*, 153–157.

Braun, S., Kalinowski, H. -O., & Berger, S. (1996). *100 and more Basic NMR experiments. A practical course*, Weinheim: VCH.

Catoire, L., Derouet, C., Redon, A. -M., Goldberg, R., & Herve du Penhoat, C. (1997). An NMR study of the dynamics of single-stranded conformation of sodium pectate. *Carbohydrate Research*, *300*, 19–29.

Craik, D. J., Kumar, A., & Levy, G. C. (1983). MOLDYN: a generalized program for the evaluation of molecular dynamics models using nuclear magnetic resonance spin-relaxation data. *Journal of Chemical Information and Computer Sciences*, *1*, 28–30.

Dais, P. (1987). Carbon-13 magnetic relaxation and local chain motion of amylose in dimethylsulfoxide. *Carbohydrate Research*, *160*, 73–93.

Dais, P. (1995). Carbon-13 nuclear magnetic relaxation and motional behavior of carbohydrate molecules in solution. *Advances in Carbohydrate Chemistry and Biochemistry*, *51*, 63–131.

Dais, P., & Marchessault, R. H. (1991). $^{13}C$ nuclear magnetic resonance relaxation of amylose and dynamic behavior of the hydroxymethyl group. *Macromolecules*, *24*, 4611–4614.

Dais, P., & Spyros, A. (1995). $^{13}C$ nuclear magnetic relaxation and local dynamics of synthetic polymers in dilute solutions and in the bulk state. *Progress in NMR Spectroscopy*, *27*, 555–633.

De Bruyn, A., Anteunis, M., & Verhegge, G. (1975). $^{1}H$ NMR study of diglucopyranoses in D2O. *Bulletin de la Societe of Chimique Belgique*, *84*, 721–734.

Dejean de la Batie, R., Lauprêtre, F., & Monnerie, L. (1988). Carbon-13 NMR investigation of local dynamics in bulk polymers at temperatures well above the glass-transition temperature. 1. Poly(vinyl methyl ether). *Macromolecules*, *21*, 2045–2052.

Doddrell, D. M., Glushko, V., & Allerhand, A. (1972). Theory of Nuclear Overhauser Enhancement and $^{13}C–^{1}H$ dipolar relaxation in proton decoupled carbon-13 NMR spectra of macromolecules. *Journal of Chemical Physics*, *56*, 3683–3689.

Doddrell, D. M., Pegg, D. T., & Bendall, M. R. (1982). Distortionless enhancement of NMR signals by polarization transfer. *Journal of Magnetic Resonance*, *48*, 323–327.

Engelsen, S. B., Mackie, W., & Perez, S. (1996). A molecular builder for carbohydrates. Application to polysaccharides and complex carbohydrates. *Biopolymers*, *39*, 417–433.

Heatley, F. (1979). Nuclear magnetic relaxation of synthetic polymers in dilute solution. *Progress in NMR Spectroscopy*, *13*, 47–85.

Isihara, A. (1968). Irreversible processes in solutions of chain polymers. *Fortschritte der Hochpolymeren-Forschung*, *5*, 531–567.

London, R. E. (1978). On the interpretation of $^{13}C$ spin–lattice relaxation resulting from ring puckering in proline. *Journal of the American Chemical Society*, *100*, 2678–2685.

London, R. E., & Avitabile, J. (1978). Calculated $^{13}C$ NMR relaxation parameters for a restricted internal diffusion model. Application to methionine relaxation in dihydrofolate reductase. *Journal of the American Chemical Society*, *100*, 7159–7165.

Rinaudo, M., & Vincendon, M. (1982). $^{13}C$ NMR structural investigation of scleroglucan. *Carbohydrate Polymers*, *2*, 135–144.

Scarsdale, J. N., Prestegard, J. H., Ando, S., Hori, T., & Yu, R. K. (1986). $^{1}H$-2D-Nuclear magnetic resonance applied to the primary structure determination of a novel octasaccharide glycolipid isolated from the spermatozoa of bivalves. *Carbohydrate Research*, *155*, 45–56.

Spyros, A., & Dais, P. (1992). Structure and dynamics of poly(1-naphthyl acrylate) in solution by $^{13}C$ NMR spectroscopy. *Macromolecules*, *25*, 1062–1067.

Spyros, A., & Dais, P. (1995a). Composite spectral density functions for the interpretation of the $^{13}C$ NMR relaxation behavior of polymers containing hydrocarbon side chains. Free and restricted side chain motion. *Journal of Polymer Science, Part B: Polymer Physics*, *33*, 353–365.

Spyros, A., & Dais, P. (1995b). Local chain motions of poly(β-hydroxyoctanoate) in the bulk. $^{13}C$ NMR relaxation study. *Journal of Polymer Science, Part B: Polymer Physics*, *33*, 353–365.

Spyros, A., Dais, P., & Heatley, F. (1994). Chain segmental motion and side-chain internal rotations of poly(1-naphthylalkyl acrylate)s in solution studied by $^{13}C$ nuclear magnetic relaxation. *Macromolecules*, *27*, 5845–5857.

Tylianakis, E., Dais, P., Andre, I., & Taravel, F. R. (1995). Rotational dynamics of linear polysaccharides in solution. $^{13}C$ Relaxation study on amylose and inulin. *Macromolecules*, *28*, 7962–7966.

Tylianakis, E., Spyros, A., Dais, P., Taravel, F. R., & Perico, A. (1999). NMR study of the rotational dynamics of linear homopolysaccharides in dilute solutions as function of linkage position and stereochemistry. *Carbohydrate Research*, *315*, 16–34.

Woessner, D. E. (1962). Nuclear spin relaxation in ellipsoids undergoing rotational Brownian motion. *Journal of Chemical Physics*, *31*, 647–654.